ARTICLE

Check for updates

A generic hierarchical model of organic matter degradation and preservation in aquatic systems

Haitao Shang [1 ✉]

Organic matter degradation and preservation are crucial components of Earth's carbon cycle. Empirical and phenomenological models usually contain parameters determined by site-specific data and focus on different aspects of the decay and accretion characteristics. To investigate more fundamental mechanisms, this study suggests a hierarchical model that links microscopic physical quantities to macroscopic degradation and preservation patterns. This mechanistic model predicts several commonly observed phenomena, including the lognormal distribution of degradation rate constants, the recalcitrance-dependent sensitivity to temperature, the dependence of a heterogeneous organic-matter system's persistence on its complexity, logarithmic-time decay, and power-law degradation behavior. The theoretical predictions of this model are consistent with the observational data from marine and lake environments. This hierarchical model may provide a step towards a fundamental theory of organic matter degradation and preservation in aquatic and other ecosystems.

[1] Institute of Ecology and Evolution, University of Oregon, Eugene, OR 97403, USA. ✉email: htshang.research@gmail.com

Earth's carbon cycle provides us a window through which to investigate the interactions between life and the environment in different spatial and temporal scales[1,2]. As two main components of the carbon cycle, oxygenic photosynthesis and organic degradation play important roles in controlling these interactions[1,2]. In oxygenic photosynthesis, photoautotrophs (e.g., plants, algae, and cyanobacteria) use water (H_2O) and carbon dioxide (CO_2) as raw materials and energy in the form of photons to produce organic matter (CH_2O) and molecular oxygen (O_2) via the forward reaction in the following chemical equation: energy + H_2O + CO_2 ⇌ CH_2O + O_2, where CH_2O is a schematic chemical formula representing a large variety of organic compounds produced by photosynthetic activities. The backward reaction (i.e., aerobic respiration) burns organic matter with O_2 and provides energy to heterotrophic organisms.

The loop between photosynthesis and respiration drives the material and energy exchanges between the biological and geological components of Earth's carbon cycle. However, there exists a tiny leak in this loop. A small amount of organic matter originating from photosynthetic activities escapes degradation and is buried in sedimentary rocks, leading to the accumulation of O_2 in Earth's atmosphere and oceans[1,2]. As a result, organic matter degradation and preservation determine the net CO_2 flux out of Earth's surface and the net O_2 flux into it.

Organic matter is highly heterogeneous[3]; so, too, is the environment in which it is deposited[4]. The complex interplay between the intrinsic molecular composition and extrinsic environmental variables influences the degradability of organic matter. In aquatic (e.g., marine and lake) systems, the chemical properties and degradation/preservation mechanisms of organic matter are altered as it sinks through the water column and accumulates in sediments[5,6]. Correspondingly, different interpretations have been proposed for the recalcitrant fraction in dissolved and sedimentary organic matter. For example, the dilution hypothesis[7–9] suggests that low concentrations of labile components in dissolved organic matter may significantly reduce the effective energy gains from microbial respiration, resulting in the recalcitrance of these organic compounds in the water column. Instead, the physical protection hypothesis[10,11] proposes that the association of sedimentary organic matter with minerals can protect the former from enzymatic attacks of microorganisms when it passes through the thermodynamic ladder[12] of redox zones in sediments, leading to the persistence of organic matter. These hypotheses offer qualitative understandings of organic matter degradation and preservation in marine and lake environments; investigating the fundamental microscopic mechanisms of degradation/preservation and predicting the long-term fates of organic matter, however, require a more quantitative theoretical framework.

Different empirical and phenomenological models[13–17] have been proposed to interpret the spatial and temporal variations of organic matter. Nevertheless, the mathematical formulations of existing models usually are not well constrained and contain parameters determined by site-specific data[18]. Moreover, studies on organic matter decay and accretion often focus on thermodynamics[12,19]; biogeochemical models considering kinetics are generally dictated by simple rate constants[13–17]. Understanding the underlying microscopic mechanisms of organic matter degradation and preservation is necessary for developing a more fundamental theory[4].

This work proposes a hierarchical model that predicts several phenomena commonly observed in previous studies, including the lognormal distribution of degradation rate constants[3,20], the recalcitrance-dependent sensitivity to temperature[21–23], the dependence of a heterogeneous organic-matter system's persistence on its complexity[24–26], logarithmic-time decay[27–29], and

power-law degradation behavior[14,30–32]. The plausible consistency of this model's predictions with the field observations in marine and lake environments suggests that the theory presented here potentially provides a step toward a fundamental theoretical framework of organic degradation and preservation in aquatic and possibly other ecosystems.

Results

A discrete hierarchical ensemble of organic matter. Previous studies have suggested a variety of physical, chemical, and biological factors determining the persistence of organic matter[4–6]. Many factors influence the decay and burial of organic compounds by affecting their reactivities and activation barriers[10,11]. For instance, the physical protection hypothesis suggests that the long-term preservation of some types of organic compounds in marine and lake sediments is a consequence of their strong association with mineral surfaces, which elevates the activation energy for degradation and prevents these organic compounds from the attacks of microbial enzymes[10,11]. Here, I suggest a hierarchical model for organic matter degradation from the perspective of kinetics (i.e., reactivity and activation energy).

I consider a hierarchical ensemble of organic compounds $\{C_i\}$ with degradation rate constant k_i, where $i \in [0, N]$, N is the highest level in the hierarchy, and C_i represents the organic matter at level i. Figure 1(a) shows a series of decay reactions occurring along a degradation coordinate: $C_N \xrightarrow{k_N} C_{N-1}, \dots, C_i \xrightarrow{k_i} C_{i-1}, \dots, C_0 \xrightarrow{k_0} CO_2$. In this hierarchical ensemble, C_N represents the most recalcitrant organic matter, which has the longest persistence, while C_0 is the most labile organic matter, which is preferentially utilized by organisms in natural environments. The activation energy for the final step on the degradation coordinate is denoted by E_0, and the activation energy for the degradation reaction occurring i steps prior to the final step is denoted by E_i. One should note that "hierarchical" here does not mean "sequential"; the degradation of organic compounds at different hierarchical levels occurs in parallel simultaneously.

The objective of this hierarchical model is to investigate the connection of organic degradation patterns to kinetics (e.g., k_i and E_i) rather than to thermodynamics (e.g., the Gibbs free energy). Thus, I assume that each reaction at level i along the degradation coordinate has a negative Gibbs free energy change (i.e., $\Delta G_i < 0$) and therefore is thermodynamically feasible. Moreover, in this hierarchical model, organic compounds having the same activation energy E_i are treated as identical component C_i located at the same hierarchical level (i.e., the i-th level) regardless of their compositions and structures.

According to the transition state theory[33,34], the rate constant for the i-th reaction is expressed by

$$k_i = \frac{k_B T}{\hbar} \exp\left(-\frac{E_i}{RT}\right) \quad (1)$$

where k_B is the Boltzmann constant, $\hbar$ is the Planck constant, T is thermodynamic temperature, and R is the ideal gas constant. Organic compounds at different hierarchical levels start to decay from distinct points on the degradation coordinate (Fig. 1(a)). Their eventual fates, however, are the same: being completely degraded to CO_2 and removed from the ensemble. I define the total activation energy for the complete degradation of organic matter at the i-th level as its effective activation energy:

$$\epsilon_i = \sum_{j=0}^{i} E_j. \quad (2)$$

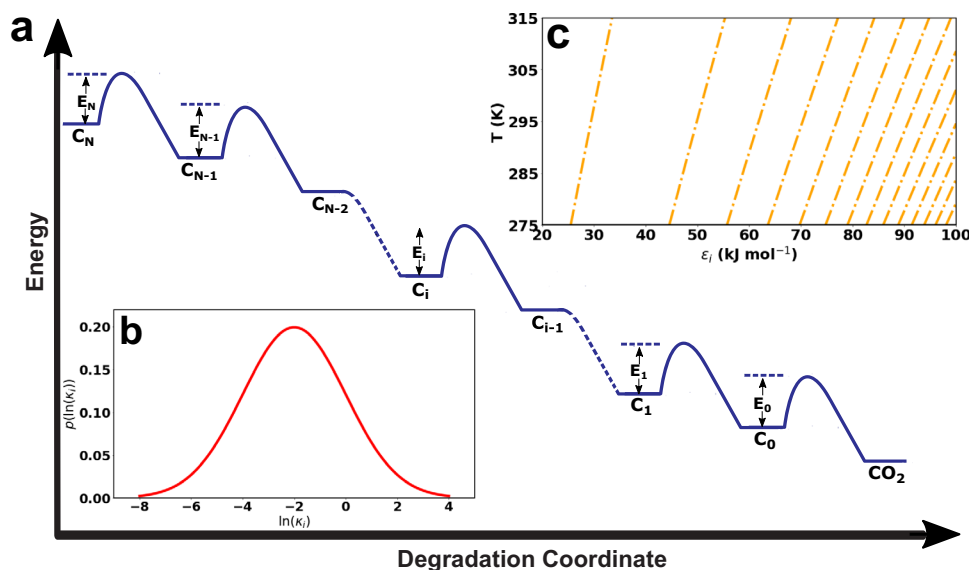Correspondingly, the effective degradation rate constant for

Fig. 1 A profile of activation energy along the discrete degradation coordinate and two direct predictions of the hierarchical model. a Activation energy profile for organic matter degradation, in which C_i represents the organic matter at level i, and E_i represents the activation energy for the i-th reaction. The energy profile illustrated here appears along a discrete degradation coordinate; its continuous form is introduced later. **b** Lognormal distribution of the effective degradation rate constant (κ_i) predicted by Eq. (4). The mean and variance of this lognormal distribution depends on the type of organic matter and the environment in which it decays. The specific distribution presented in panel **b** is for the degradation rate constants of plant biomass[3]. **c** Recalcitrance-dependent sensitivity to temperature predicted by Eq. (5). The orange contours represent the temperature sensitivity of rate constants (i.e., $\partial \kappa_i / \partial T$). When organic matter is more recalcitrant (i.e., the effective activation energy, ϵ_i, is higher), its degradation responds more sensitively to the changes in temperature.

organic matter at the i-th level is defined as

$$\kappa_i = \frac{k_B T}{\hbar} \exp\left(-\frac{\epsilon_i}{RT}\right). \tag{3}$$

I substitute Eqs. (1) and (2) into Eq. (3), apply the product rule for exponents, and obtain $\kappa_i = (k_B T/\hbar) \exp\left[-\sum_{j=0}^{i} E_i/(RT)\right] \sim \prod_{j=0}^{i} k_j$.

Two direct predictions of the hierarchical model. From the perspective of stochastic reaction kinetics[35,36], k_j represents the probability per unit time that the i-th reaction on the degradation coordinate (i.e., the transformation of organic matter from the j-th level to the $(j-1)$-th level) will occur. Therefore, κ_i represents the probability per unit time that organic matter at the i-th level will completely decay to CO_2. The above relation between the effective rate constant (κ_i) and conventional rate constant (k_j) can be rewritten as $\ln \kappa_i \sim \sum_{j=0}^{i} \ln k_j$. Because (i) organic matter degradation usually consists of plenty of steps to complete (i.e., $1 \ll i$) and (ii) k_m and k_n are independent for $m \neq n$, the Central Limit Theorem implies that κ_i satisfies a lognormal distribution[37,38]:

$$\ln \kappa_i \hookrightarrow \mathcal{N}(\mu_i, \sigma_i^2) \tag{4}$$

where $\mathcal{N}$ is a normal distribution with mean $\mu_i \sim \sum_{j=0}^{i} \mathbb{E}(\ln k_j)$ and variance $\sigma_i^2 \sim \sum_{j=0}^{i} \mathrm{Var}(\ln k_j)$. This result (Eq. (4)), a particular case of which appears in Fig. 1(b), is consistent with previous theories and observations[3,20] and suggests an alternative interpretation for the origin of the lognormal distribution of organic matter degradation rate constants.

The other direct prediction of the hierarchical model is the recalcitrance-dependent sensitivity to temperature. The relative sensitivity of the organic matter degradation rate at the i-th

hierarchical level to temperature can be expressed as

$$\frac{\partial \ln \kappa_i}{\partial T} = \frac{1}{T}\left(1 + \frac{\epsilon_i}{RT}\right). \tag{5}$$

This equation, also illustrated in Fig. 1(c), shows that, when organic matter has higher effective activation energy, the dependency of its degradation rate on temperature is stronger. This relation is consistent with a phenomenon observed in previous studies[21–23]: the decay of more recalcitrant organic matter responds more sensitively to changes in temperature.

Organic matter degradation and preservation on a continuum. As discussed above, in the hierarchical model, organic compounds having the same activation energy E_i are treated as identical component C_i; they are initially located at the i-th level and start to decay from this position. I assume that the activation barrier for the i-th decay reaction consists of n_i barrier units and denote the activation energy of each barrier unit by Δu. The activation energy at the i-th reaction then can be written as

$$E_i = n_i \Delta u. \tag{6}$$

I denote the initial total amount of organic matter in the whole hierarchical ensemble $\{C_i\}$ by G_0, and the fraction of organic matter at the i-th level (i.e., with n_i activation barriers) by f_i; the initial amount of component C_i then is expressed as $G_0 f_i$. I assume that barrier units are uniformly distributed at each hierarchical level along the degradation coordinate, implying that n_i is proportional to C_i amount and therefore $f_i \simeq n_i / \sum_{j=0}^{N} n_j$. Following the conventional first-order kinetics[13–15], the amount of leftover C_i after t is expressed by $g_i(t) = G_0 f_i \exp(-\kappa_i t)$. The ensemble consists of N hierarchical levels; thus, there are N different degradation processes occurring in parallel simultaneously. Therefore, the total amount of remaining organic compounds in the whole ensemble at time t is $G(t) = \sum_{i=0}^{N} g_i(t)$, and the preservation efficiency is defined as $B(t) = G(t)/G_0$. I substitute Eqs.

(1)–(3) and (6) into this definition of $B(t)$ and express the preservation efficiency of the whole ensemble as a linear superposition of the fractions of leftover organic matter at each hierarchical level:

$$B(t) = \sum_{i=0}^{N} \left(\frac{n_i}{\sum_{j=0}^{N} n_j} \right) \left(\exp\left[-\kappa_0 t \exp\left(-\frac{\epsilon_{\max}}{RT} \frac{\sum_{j=0}^{i} n_j}{\sum_{j=0}^{N} n_j} \right) \right] \right) \quad (7)$$

where $\epsilon_{\max} = \sum_{i=0}^{N} E_i$ is the effective activation energy at the highest hierarchical level. Eq. (7) links the macroscopic quantity B to the microscopic quantities n_i and $\epsilon_{\max}$ on a discrete degradation coordinate.

Theoretical studies[4,14,15] and laboratory/field observations[39,40] have suggested that organic matter in natural environments can be represented by a continuum of species with a wide range of reactivities. Compared to the discrete coordinate (Fig. 1(a)) from which Eq. (7) is derived, a continuous coordinate, which is henceforth called a degradation continuum, would provide a more realistic depiction of the degradation path[4]. In such a scenario, the summation in Eq. (7) can be rewritten as an integral. To do so, I first assume that the number of activation barrier units (n_i) changes smoothly with i along the degradation coordinate (Fig. 1(a)). This assumption allows us to introduce an (almost) continuous variable $x_i = n_i \delta$, where $\delta \ll 1$. I define a function $\tilde{f}(x_i)$ to represent the fraction of the continuous variable x_i over the summation of x_i on all N levels: $\tilde{f}(x_i) = x_i / \sum_{j=0}^{N} x_j$, which is analogous to the function f_i for the discrete variable n_i. The fraction of organic matter that has effective activation energy up to level i on the degradation continuum then can be expressed by $\int_{x_0}^{x_i} \tilde{f}(x')dx'$. To obtain the mathematical expression of $B(t)$ on the degradation continuum from Eq. (7), I introduce a variable $s = \int_{x_0}^{x_i} \tilde{f}(x')dx' / \int_{x_0}^{x_{\max}} \tilde{f}(x')dx'$ (the Methods section), where $x_{\max} = N\delta$. This variable s is the normalized, continuous form of $(\sum_{j=0}^{i} n_j)/(\sum_{j=0}^{N} n_j)$; the denominator $\int_{x_0}^{x_{\max}} \tilde{f}(x')dx'$ in s is a normalization factor that guarantees $0 \le s \le 1$ (the Methods section). Eq. (7) then can be rewritten as the following integral form (the Methods section): $B(t) = \int_0^1 \exp\left(-\kappa_0 t \exp\left[-(\epsilon_{\max}s)/(RT)\right]\right)ds$. Further calculation (the Methods section) transforms this integral to an expression for $B(t)$ in terms of integral exponential functions:

$$B(t) = \frac{RT}{\epsilon_{\max}} \left[\text{Ei}\left(\frac{t}{\tau_N}\right) - \text{Ei}\left(\frac{t}{\tau_0}\right) \right] \quad (8)$$

where $\tau_N = 1/\kappa_N$ and $\tau_0 = 1/\kappa_0$ are the length of time for the most recalcitrant and the most labile organic compounds, respectively, in the ensemble to completely decay to CO_2, and $\text{Ei}(x) = \int_x^{\infty} \left[\exp(-t)/t \right]dt$.

The preservation efficiency, B, in Eq. (8) is characterized by four parameters: τ_0 and τ_N determine the time scales, and $\epsilon_{\max}$ and T determine the functional shape of B. It is important to note that τ_0 and τ_N are functions of T and $\epsilon_{\max}$ (Eq. (3)); therefore Eq. (8) does not simply claim that B is positively correlated with T while negatively correlated with $\epsilon_{\max}$. In contrast, as demonstrated in the Methods section, B depends negatively on T and positively on $\epsilon_{\max}$. The negative correlation between B and T is consistent with a broadly observed phenomenon: an increase in temperature would promote the remineralization of organic matter, resulting in less preservation[41,42]. In the following sections, I show that several commonly observed phenomena of organic matter degradation and preservation can be derived from Eq. (8) and that the theoretical predictions are consistent with observational data from aquatic systems.

Logarithmic oxygen-exposure-time decay. In oxic environments, t in Eq. (8) is conventionally interpreted as oxygen exposure time (t_{O_2})[27,28], that is, the length of time during which
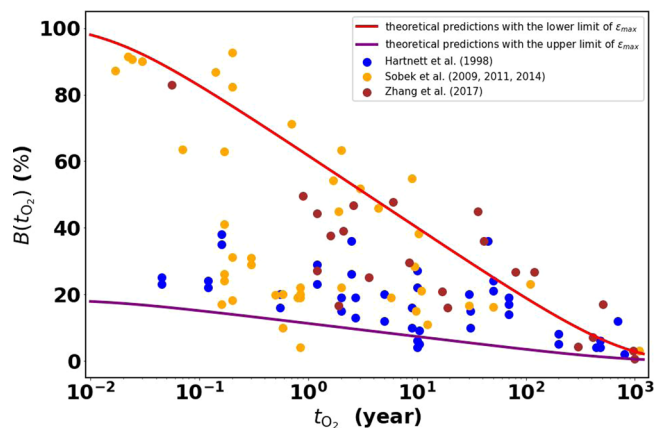

Fig. 2 Theoretical predictions (red and purple curves) and field observations (circles) of the relation between preservation efficiency (B) and oxygen-exposure time (t_{O_2}) in sediments. Data are compiled from the studies by Hartnett et al.[28] (blue), Sobek et al.[27,43,44] (orange), and Zhang et al.[29] (brown). The two theoretical curves are predicted by Eq. (8) with $\tau_0 = 10^{-2}$ year (i.e., the minimum oxygen-exposure time in the data), $\tau_N = 10^3$ year (i.e., the maximum oxygen-exposure time in the data), $T = 288$ K (i.e., the average temperature of oxic sediments on the surface of continental shelves and lake bottoms[41,45]), and $\epsilon_{\max} = 25$ kJ/mol (the lower limit of $\epsilon_{\max}$) or $\epsilon_{\max} = 140$ kJ/mol (the upper limit of $\epsilon_{\max}$). The theoretical predictions corresponding to $\epsilon_{\max}$ values between the lower and upper limits fall between these two curves.

organic matter is exposed to O_2. Oxygen exposure time has been suggested as a proxy for the aerobic degradation of organic matter[27,28]. Figure 2 shows the data on "preservation efficiency versus oxygen-exposure time" in sediments (circles) compiled from field observations[27–29,43,44], which are used to test the theoretical relation between B and t_{O_2} in Eq. (8). These data are measured from the sediments deposited on the surface of continental shelves or lake bottoms, where most of the organic matter burial on Earth takes place[1,10]. The temperature of such environments usually varies from 273 K to 303 K with an average of 288 K[41,45]. The timescale of the compiled data ranges from 10^{-2} to 10^3 years; I assume that τ_0 and τ_N in Eq. (8) equal 10^{-2} and 10^3 years, respectively. Supplementary Table 1 summarizes the activation energy for organic matter degradation in marine and lake sediments. According to these data, I take 25 kJ/mol and 140 kJ/mol as the lower and upper limits of $\epsilon_{\max}$, respectively. Figure 2 displays the theoretical relation between B and t_{O_2} predicted by Eq. (8). The red and purple curves represent the predictions with the lower and upper limits of $\epsilon_{\max}$, respectively; more than 85% of the compiled data fall in the region between them (Fig. 2). These curves are obtained without fitting free parameters, which is different from the traditional approaches in which models with free parameters (e.g., linear regression)[27,28,43,44] are used to fit the empirical relation between B and t_{O_2}.

Based on the data in Fig. 2, previous studies[27–29,43,44] have suggested that the preservation efficiency of organic matter in marine and lake sediments is a monotonically decreasing function of the logarithm of oxygen-exposure time. Here, I show that logarithmic-t_{O_2} decay of organic matter can be derived from Eq. (8). In natural environments, highly labile organic compounds decay in several minutes or even shorter, while extremely recalcitrant organic compounds can be stored for millions of years or even longer[4,46]. Asymptotic analysis of Eq. (8) (the Methods section) shows that, when degradation time t_{O_2} falls between its lower and upper limits (i.e., $\tau_0 \ll t_{O_2} \ll \tau_N$),

preservation efficiency in sediments can be written as the following asymptotic form:

$$B(t_{O_2}) \simeq 1 - 2.3\log_{10}\left(\frac{t_{O_2}}{\tau_0}\right)\frac{RT}{\epsilon_{max}} \qquad (9)$$

which suggests that the slope of preservation efficiency in sediments versus oxygen-exposure time depends on ϵ_{max} and T. The logarithmic-t_{O_2} decay shown in Eq. (9) effectively ceases at time τ_N because the $B(t_{O_2}) \simeq 0$ when $t_{O_2} \gg \tau_N$ (the Methods section). This theoretical logarithmic-t_{O_2} decay pattern (Eq. (9)) is consistent with the empirical relations suggested by previous studies[27–29,43,44], indicating that the hierarchical model provides insights into the underlying mechanisms of organic matter decay and accretion in marine and lake sediments.

Dependence of an organic-matter system's persistence on its complexity. By definition, the preservation efficiency function $B(t)$ represents the fraction of the organic matter at age t (i.e., the waiting time before degradation occurs), where $t = 0$ is set at the time point when organic matter initially arrives in ocean or lake. Field studies have shown that the age of organic matter ranges from a few minutes (or even shorter) to millions of years (or even longer)[4,46]. Here, I assume that the length of the degradation time for organic compounds in the hierarchical ensemble varies from 0 to ∞. As shown in the Methods section, $B(t) \rightarrow 1$ as $t \rightarrow 0$ while $B(t) \rightarrow 0$ as $t \rightarrow \infty$. These two limits are consistent with the physical definition of $B(t)$ as a ratio between the remaining and initial amounts of organic matter: this ratio can be no higher than 1 because secondary production always comes at the expense of degradation of other organic compounds and will reach 0 when all organic matter is consumed. Since $B(t)$ ranges from 0 to 1, it also represents the cumulative distribution function (starting at $t = \infty$) of the ages of organic compounds in the ensemble, and the corresponding probability density function $p(t)$ is $p(t) = |dB(t)/dt|$. The average age of all organic compounds in the hierarchical ensemble, $\langle t \rangle = \int_0^\infty tp(t)dt$, is then expressed as

$$\langle t \rangle \propto \exp\left(\frac{\epsilon_{max}}{RT}\right)\tau_0 \qquad (10)$$

in which $\langle \cdot \rangle$ represents the average of a quantity. The derivation of Eq. (10) is provided in the Methods section.

The relation in Eq. (10) suggests that the average age of an organic-matter system increases with its maximum effective activation energy, which depends on the complexity of this system. When the complexity of composition (e.g., molecular diversity) and the environment (e.g., spatial heterogeneity and temporal variability) rises, the number of parallel degradation processes and thus the total number of hierarchical levels (N) will also increase. This growth of N would lead to a higher ϵ_{max} because $\epsilon_{max} = \sum_{i=0}^N n_i \Delta u$. Consequently, the ensemble of organic matter rewards less energy to microbial metabolisms[47] and therefore has a longer average age $\langle t \rangle$. In other words, Eq. (10) suggests that an organic-matter ensemble with higher complexity tends to be more persistent, which is consistent with previous observations in aquatic systems[24–26].

Power-law degradation behavior. To investigate how the degradation kinetics change with time, I express the degradation of the whole hierarchical ensemble in terms of the conventional first-order kinetics[13–15]: $dG(t)/dt = -K(t)G(t)$, where $K(t)$ is the average degradation rate constant of all organic compounds in the ensemble. When the length of time (i.e., age) t is within the

Table 1 Parameter values in the power-law relation, $\log_{10} K = -a\log_{10} t + b$, in published studies.

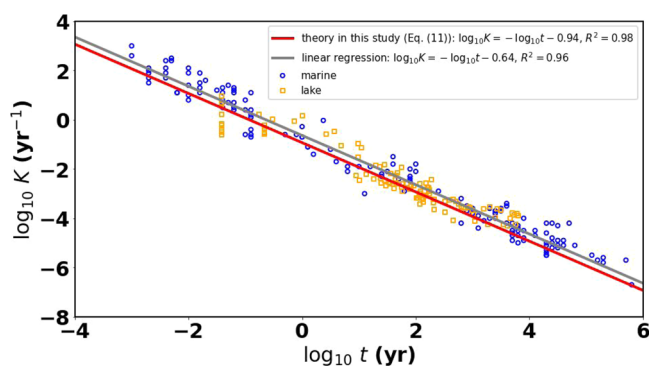| a	b	Environment	Method	Reference
0.95	-0.81	Marine	Linear regression	Middelburg[14]
0.99	-0.68	Marine	Linear regression	Middelburg et al.[30]
1.21	-	Marine	Linear regression	Beulig et al.[31]
0.98	-0.31	Lake (oxic)	Linear regression	Katsev and Crowe[32]
0.86	-1.10	Lake (anoxic)	Linear regression	Katsev and Crowe[32]
1	System-dependent	Various	A hierarchical model	This study

Fig. 3 Theoretical prediction and field data for the power-law relation between organic carbon reactivity (K) and age (t) in marine and lake systems. Blue circles and orange squares represent data from marine[30] and lake systems[32], respectively. Red and grey straight lines are the theoretical approximation of Eq. (11) and linear regression, respectively, for the data from both marine and lake environments. R^2 represents the coefficient of determination of the theoretical approximation or linear regression.

two extreme timescales, that is, $\tau_0 \ll t \ll \tau_N$, I have

$$\log_{10} K = -\log_{10} t + b, \text{ where } b = \log_{10}\left[\exp\left(-\frac{t}{\tau_N}\right)\Big/\text{Ei}\left(\frac{t}{\tau_N}\right)\right]. \qquad (11)$$

The derivation of Eq. (11) is provided in the Methods section. On a log-log graph, the relation between K and t in Eq. (11) is represented by a straight line with a slope of -1 and an intercept of b, which is consistent with the power-law behavior shown by the previous observations[14,30–32]: $\log_{10} K = -a\log_{10} t + b$.

Table 1 summarizes the values of a and b obtained by empirical studies from marine[14,30,31] and lake[32] environments and predicted by the hierarchical model in this study. The theoretical value of a equals 1; this result is consistent with the empirical values of a, which approximate 1, from field studies[14,30–32]. The value of b, however, varies in a relatively large range. The system-dependent variation of b values demonstrated in Table 1 may be explained by the dependence of b on τ_N shown in Eq. (11): the factors influencing τ_N and therefore b, such as organic matter composition and environmental conditions, change across the observation sites in these studies[14,30,32].

Data (blue circles and orange squares in Fig. 3) measured from the marine[30] and lake[32] systems are compiled to test the predictions of Eq. (11). To obtain the theoretical estimate of intercept b over these data, I first determine the value of the characteristic degradation time τ_N. The minimum degradation rate constant in the compiled dataset (Fig. 3) is $K_{min} \simeq 2 \times 10^{-7}$ year^{-1}, implying that

$\tau_N = 1/K_{\min} \simeq 5 \times 10^6$ year. I substitute this τ_N value into Eq. (11) and calculate the average of $\log_{10}\left[\exp(-t/\tau_N)/\mathrm{Ei}(t/\tau_N)\right]$ over t of the data in Fig. 3; this average, -0.94, is the theoretical estimate of b for the compiled dataset. The red line ($\log_{10}K = -\log_{10}t - 0.94$; $R^2 = 0.98$) in Fig. 3 shows this theoretical relation, while the grey line ($\log_{10}K = -\log_{10}t - 0.64$; $R^2 = 0.96$) in Fig. 3 is obtained via linear regression, which is the conventional method used in the previous studies[30,32]. The theoretical line has a coefficient of determination (R^2) that is as good as the linear-regression line. Given that the value of b is system-dependent, I apply the same analyses to marine data or lake data individually to test if the predictions by Eq. (11) hold for separate, smaller datasets. The results, which are presented in Supplementary Figure 1 and Supplementary Table 2, show that the theoretical formula still performs as well as or even better than the traditional linear-regression method.

Relating organic preservation hypotheses to the hierarchical model. The results presented in previous sections (Eqs. (9), (10), and (11)) show that the patterns of organic matter decay and accretion are primarily constrained by the lower and upper extremes of effective activation energy in the hierarchical ensemble: ϵ_0 and $\epsilon_{\max}$ (note that κ_0, κ_N, τ_0 and τ_N are all functions of ϵ_0 or $\epsilon_{\max}$). This suggests that the degradation and preservation of organic matter are influenced by three microscopic quantities in the hierarchical model, N, Δu, and n (Eqs. (2) and (6)), which characterize an organic-matter ensemble's complexity, the energy of each barrier unit, and the number of unit barriers at each hierarchical level, respectively. These physical quantities potentially shed light on the underlying mechanisms of organic matter decay and persistence.

Figure 4 illustrates the possible connections of the three microscopic quantities in the hierarchical model with several hypotheses of organic matter preservation. Each of these hypotheses can be characterized by either one quantity or a combination of multiple quantities. For example, the complexity hypothesis[24–26] is represented in hierarchical model by N. As the complexity (e.g., the molecular diversity, spatial heterogeneity, and temporal variability) of an organic-matter ensemble rises, its retention time (i.e., age) becomes longer. Other explanations for the long-term preservation of organic matter, including intrinsic recalcitrance (e.g., inherent qualities of organic matter)[4–6], external environments (e.g., physical and chemical factors shaping microbial communities)[4–6], and physical protection (e.g., mineral-organic matter association)[10,11], are characterized by $n\Delta u$ in the hierarchical model. As these factors become stronger, $n\Delta u$ increases, leading to a more persistent organic-matter ensemble.

The conceptual diagram in Fig. 4 provides a primitive but plausible approach to link microscopic quantities to the existing hypotheses of organic preservation. However, this framework requires further theoretical validation and experimental tests. Moreover, the hierarchical model is based on the classical theory of chemical kinetics; incorporating quantities/principles from thermodynamics (e.g., Gibbs free energy[12,19]) and quantum statistics (e.g., Fermi-Dirac statistics[48]) into the current model may offer deeper insights into more fundamental mechanisms of organic matter degradation and preservation.

Discussion

The degradation and preservation of organic matter appears to be a complex process because its underlying mechanisms have not been well understood[4]. Occam's razor[49] and the simplicity postulate[50] both point in the direction of developing simple models and evaluating their predictions. From the perspective of kinetics, this study develops a hierarchical model to depict organic matter decay and accretion and predicts several
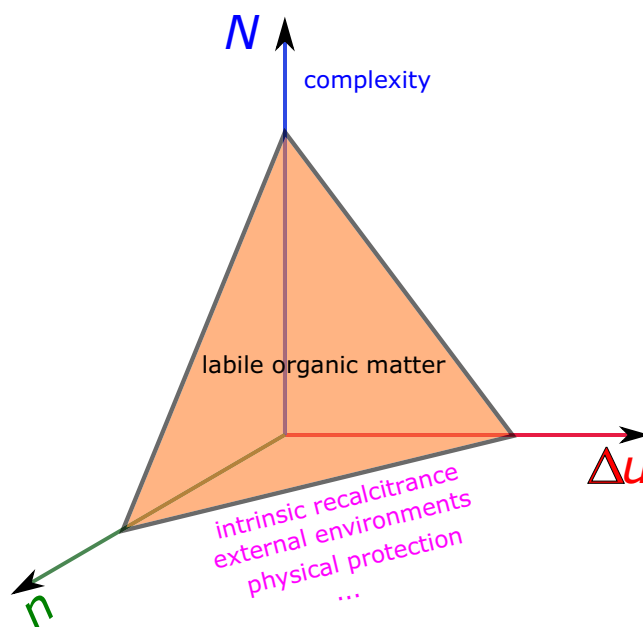

Fig. 4 A conceptual diagram of the connections between three microscopic quantities (N, Δu, and n) and organic matter preservation hypotheses. Quantity N represents an organic-matter ensemble's complexity, Δu is the energy of each barrier unit, and n characterizes the number of unit barriers at each hierarchical level. Quantity N is related to the complexity hypothesis; $n\Delta u$ is linked to several hypotheses, including intrinsic recalcitrance, external environments, and physical protection. When N, n, and Δu of an organic matter system are all relatively small (i.e., inside the orange tetrahedral region), it tends to be labile. In contrast, an ensemble of organic matter is recalcitrant when one or more of N, n, and Δu are higher than some thresholds (i.e., outside the orange tetrahedral region).

commonly observed phenomena; in particular, this model provides excellent predictions that correspond to logarithmic-t_{O_2} decay[27–29] and power-law degradation behavior[14,30–32]. The consistency between theoretical predictions and observational data in marine and lake environments suggests that this hierarchical model potentially offers a framework for a fundamental theory of organic matter degradation and preservation in aquatic and possibly other ecosystems.

There are a variety of valid approaches for modeling organic matter decay[13–17]. Particularly, the mathematical form of Eq. (11) in this study is identical to that of Eq. (5) in the theory of Rothman and Forney[16], which presents a reaction-diffusion model for the degradation of mineral-associated organic matter in the porous marine sediments. Nevertheless, these two formulas are obtained with different physical assumptions and via distinct mathematical derivations. The model of Rothman and Forney[16] made an assumption that reactivity k of organic matter satisfies a special probability distribution $p(k) \sim 1/k$ and obtained its Eq. (5) from the connection of reactivities to reaction-diffusion dynamics. These differ from the assumptions of hierarchical structures (the Results section) and the mathematical approach of deriving Eq. (11) (the Methods section) in this study.

I do not claim that the hierarchical model is superior to the previous models. This is not only because models for any open natural system are nonunique, but also because models, even partially confirmed, have their own heuristic values[51]. However, I have found that, compared to previous empirical and phenomenological models[13–17], the hierarchical model provides an alternative approach to depict organic degradation and

preservation from a mechanistic perspective. Although some quantities, such as activation energy, have been widely applied to investigate organic matter's fate in natural environments, this work mathematically connect these quantities to logarithmic-time decay (Eq. (9)) and power-law degradation behavior (Eq. (11)) and shows plausible consistency of theory with observations.

This study mainly focuses on the geochemical aspects of organic matter degradation/preservation and develops the hierarchical model on the basis of the traditional first-order kinetics, in which the biological factors are implicitly integrated into the first-order rate constants (i.e., κ_i's). Although the hierarchical model offers a potential theoretical framework to link the chemically-oriented hypotheses for the persistence of recalcitrant organic matter (Fig. 4) to microscopic physical quantities, providing insights into the biological-oriented explanations for recalcitrance, such as the dilution hypothesis[7–9], is beyond the ability of the hierarchical model. As introduced above, the dilution effect, which derives from the imbalance between microbial respiration and its energy rewards from dilute substrates, is basically independent of the chemical properties of organic matter and therefore is not covered by the geochemically-based theoretical framework in this work.

Similar to the hierarchical model presented here, studies on organic matter decay in the water column and sediments[13–17] often formulate models using the first-order kinetics with simplistic assumptions that microbial consumers are present in sufficient numbers and thus degradation processes are independent of the abundance of microorganisms. Microbial populations and metabolisms, however, significantly influence the fates of organic matter in the water column[24,52,53] and sediments[5,6,18] in aquatic systems and therefore deserve separate treatment in future work. Explicitly incorporating biological factors into the theoretical framework proposed in this work may provide a better understanding and justification of the biologically-oriented interpretations for the persistence of recalcitrant organic matter.

Due to the limited availability of data, I tested only the predictions of logarithmic-t_{O_2} decay and power-law degradation behavior using the measurements from marine and lake environments. The fundamental mechanisms in Earth's carbon cycle, however, should be universal[4,54]; the results here (Eqs. (9), (10), and (11)) therefore are expected to apply to organic matter degradation and preservation in other ecosystems. Examining these theoretical predictions in other environments, such as soils[55,56] and rivers[57,58], may provide further support for the theory presented in this study. Moreover, several measurable indices, such as amino acid and amino sugar compositions, have been suggested as proxies for the degradation states of organic matter[59–61]; these degradation states are analogous to the hierarchical levels in the degradation coordinate (Fig. 1(a)). Researching the relations between activation energy/reactivity and decay patterns of organic matter in different degradation states (measured using those indices) would offer valuable validation for the hierarchical model and its theoretical predictions.

Hierarchical structures are ubiquitous in nature[62], implying potentially wide applications of the theory in this work. For example, many synthetic polymers (e.g., plastics) possess similar molecular structures and compositions, backbone linkages, and degradation mechanisms to those of natural organic matter[63,64]. Investigating synthetic polymers using the hierarchical model would yield insights into their decay and accretion patterns and offer clues to develop more effective, environmentally friendly management of polymer wastes. Furthermore, this study focuses on organic matter degradation and preservation in modern environments; their underlying mechanisms, however, are expected to have been the same or similar on the ancient Earth[1,2].

Incorporating the theoretical results presented here, especially the preservation efficiency function, with geochemical identification of the specific types of buried organic compounds in deep time and laboratory measurements of their effective activation energy, into global-scale biogeochemical models[65,66] may provide new perspectives on significant events in the evolution of Earth's carbon and oxygen cycles, such as carbon isotope excursions[67,68] and atmosphere-ocean oxygenation[69,70], over geologic timescales.

Methods

Preservation efficiency on a degradation continuum. In the Results section, I defined $x_i = n_i \delta$ and $\widetilde{f}(x_i) = x_i / \sum_{j=0}^{N} x_j$, where $\delta \ll 1$; therefore

$$
\begin{aligned}
\frac{\sum_{j=0}^{i} n_j}{\sum_{j=0}^{N} n_j} &= \sum_{j=0}^{i} \left(\frac{n_j \delta}{\sum_{j=0}^{N} n_j \delta} \right) \bigg/ \sum_{j=0}^{N} \left(\frac{n_j \delta}{\sum_{j=0}^{N} n_j \delta} \right) \\
&= \sum_{j=0}^{i} \left(\frac{x_j}{\sum_{j=0}^{N} x_j} \right) \bigg/ \sum_{j=0}^{N} \left(\frac{x_j}{\sum_{j=0}^{N} x_j} \right) \\
&= \sum_{j=0}^{i} \widetilde{f}(x_j) \bigg/ \sum_{j=0}^{N} \widetilde{f}(x_j).
\end{aligned}
\tag{12}
$$

On the degradation continuum, the ratio between the two summations in Eq. (12) can be written as a ratio between two integrals:

$$
\frac{\sum_{j=0}^{i} n_j}{\sum_{j=0}^{N} n_j} \longrightarrow \left(\int_{x_0}^{x_i} \widetilde{f}(x')dx' \right) \bigg/ \left(\int_{x_0}^{x_{\max}} \widetilde{f}(x')dx' \right) \equiv s
\tag{13}
$$

in which the integral over $[x_0, x_{\max}]$, i.e., $\int_{x_0}^{x_{\max}} \widetilde{f}(x')dx'$, is a normalization factor and the "$\equiv$" sign means that the variable $s \in [0, 1]$ is defined as the ratio between the two integrals.

According to the first fundamental theorem of calculus[71], I express the first derivative of s with respect to x_i as

$$
\begin{aligned}
\frac{ds}{dx_i} &= \frac{d}{dx_i} \left[\left(\int_{x_0}^{x_i} \widetilde{f}(x')dx' \right) \bigg/ \left(\int_{x_0}^{x_{\max}} \widetilde{f}(x')dx' \right) \right] \\
&= \frac{1}{\int_{x_0}^{x_{\max}} \widetilde{f}(x')dx'} \left[\frac{d}{dx_i} \left(\int_{x_0}^{x_i} \widetilde{f}(x')dx' \right) \right] \\
&= \frac{\widetilde{f}(x_i)}{\int_{x_0}^{x_{\max}} \widetilde{f}(x')dx'}.
\end{aligned}
\tag{14}
$$

With Eqs. (13) and (14), I rewrite Eq. (7) as

$$
\begin{aligned}
B(t) &= \int_{x_0}^{x_{\max}} \frac{\widetilde{f}(x_i)}{\int_{x_0}^{x_{\max}} \widetilde{f}(x')dx'} \left(\exp\left[-\kappa_0 t \exp\left(-\frac{\epsilon_{\max}}{RT} \frac{\int_{x_0}^{x_i} \widetilde{f}(x')dx'}{\int_{x_0}^{x_{\max}} \widetilde{f}(x')dx'} \right) \right] \right) dx_i \\
&= \int_0^1 \frac{\widetilde{f}(x_i)}{\int_{x_0}^{x_{\max}} \widetilde{f}(x')dx'} \left(\exp\left[-\kappa_0 t \exp\left(-\frac{\epsilon_{\max}}{RT} s \right) \right] \right) \left(\frac{\widetilde{f}(x_i)}{\int_{x_0}^{x_{\max}} \widetilde{f}(x')dx'} \right)^{-1} ds \\
&= \int_0^1 \exp\left[-\kappa_0 t \exp\left(-\frac{\epsilon_{\max}}{RT} s \right) \right] ds.
\end{aligned}
\tag{15}
$$

Finally, I derive Eq. (8) from Eq. (15):

$$
\begin{aligned}
B(t) &= \int_0^1 \exp\left[-\kappa_0 t \exp\left(-\frac{\epsilon_{\max}}{RT} s \right) \right] ds \\
&= \int_0^1 \exp\left[-\kappa_0 t \exp\left(-\frac{\epsilon_{\max}}{RT} s \right) \right] \left(-\frac{RT}{\epsilon_{\max}} \right) \exp\left(\frac{\epsilon_{\max}}{RT} s \right) \cdot d\left[\exp\left(-\frac{\epsilon_{\max}}{RT} s \right) \right] \\
&= \left(-\frac{RT}{\epsilon_{\max}} \right) \int_1^{\exp(-RT/\epsilon_{\max})} \exp(-\kappa_0 t v) \frac{1}{v} dv \\
&= \left(-\frac{RT}{\epsilon_{\max}} \right) \int_{\kappa_0 t}^{\exp(-\kappa_0 t RT/\epsilon_{\max})} \exp(-w) \frac{1}{w} dw \\
&= \left(-\frac{RT}{\epsilon_{\max}} \right) \left[\int_{\infty}^{\exp(-\kappa_0 t RT/\epsilon_{\max})} \exp(-w) \frac{1}{w} dw + \int_{\kappa_0 t}^{\infty} \exp(-w) \frac{1}{w} dw \right] \\
&= \left(\frac{RT}{\epsilon_{\max}} \right) \left[\int_{\exp(-\kappa_0 t RT/\epsilon_{\max})}^{\infty} \exp(-w) \frac{1}{w} dw - \int_{\kappa_0 t}^{\infty} \exp(-w) \frac{1}{w} dw \right] \\
&= \frac{RT}{\epsilon_{\max}} \left[\mathrm{Ei}\left(k_0 t \exp\left(-\frac{\epsilon_{\max}}{RT} \right) \right) - \mathrm{Ei}(k_0 t) \right]
\end{aligned}
\tag{16}
$$

where $\mathrm{Ei}(\cdot)$ is defined as

$$
\mathrm{Ei}(x) = \int_x^{\infty} \frac{\exp(-t)}{t} dt, \quad t \in \mathbb{R}^*
\tag{17}
$$

in which $\mathbb{R}^*$ represents non-zero real numbers. Eq. (17) is an integral exponential function.

In the above derivation, two variables $\nu = \exp[-(\epsilon_{max}s)/(RT)]$ and $\omega = \kappa_0 t\nu$ are introduced for "integration by substitution". With the definitions of effective activation energy and effective degradation rate constant (Eqs. (2) and (3)), the last line of Eq. (16) can be rewritten as Eq. (8).

The dependence of B on T and ϵ_{max}. Rewriting the discrete form of the preservation efficiency (Eq. (7)) to its continuous form (Eq. (8)) does not change the intrinsic characteristics of the preservation efficiency function itself. Here, I use the discrete form (Eq. (8)) to investigate the dependence of the preservation efficiency B on temperature T and the maximum effective activation energy ϵ_{max}. With Eqs. (1) and (3), the expression of B in Eq. (7) can be rewritten as

$$B(t) = \sum_{i=0}^{N} f_i \exp\left[-\frac{k_B T}{\hbar} \exp\left(-\frac{\epsilon_0}{RT}\right)t \exp\left(-\frac{\epsilon_{max}}{RT}f_i\right)\right]. \quad (18)$$

Then I take the partial derivatives of B with respect to T and ϵ_{max}:

$$\frac{\partial B}{\partial T} = \sum_{i=0}^{N} \frac{\partial}{\partial T}\left(f_i \exp\left[-\frac{k_B T}{\hbar} \exp\left(-\frac{\epsilon_0}{RT}\right)t \exp\left(-\frac{\epsilon_{max}}{RT}f_i\right)\right]\right)$$
$$= -\frac{1}{\hbar RT}\sum_{i=0}^{N} f_i \exp\left[-\frac{k_B Tt}{\hbar}\exp\left(-\frac{\epsilon_0 + \epsilon_{max}f_i}{RT}\right) - \frac{\epsilon_0 + \epsilon_{max}f_i}{RT}\right]k_B t(\epsilon_0 + \epsilon_{max}f_i + RT) \quad (19)$$

and

$$\frac{\partial B}{\partial \epsilon_{max}} = \sum_{i=0}^{N} \frac{\partial}{\partial \epsilon_{max}}\left(f_i \exp\left[-\frac{k_B T}{\hbar}\exp\left(-\frac{\epsilon_0}{RT}\right)t\exp\left(-\frac{\epsilon_{max}}{RT}f_i\right)\right]\right)$$
$$= \frac{k_B t}{\hbar R}\sum_{i=0}^{N} f_i^2 \exp\left[-\frac{k_B tT}{\hbar}\exp\left(-\frac{\epsilon_0 + \epsilon_{max}f_i}{RT}\right) - \frac{\epsilon_0 + \epsilon_{max}f_i}{RT}\right]. \quad (20)$$

Since the exponential function $\exp(\cdot)$ is always positive, Eqs. (19) and (20) imply

$$\frac{\partial B}{\partial T} < 0 \quad \text{and} \quad \frac{\partial B}{\partial \epsilon_{max}} > 0. \quad (21)$$

These two inequalities show that B is negatively correlated with T but positively correlated with ϵ_{max}.

Asymptotic analyses of $B(t)$. There are two timescales in Eq. (8): the long timescale determined by τ_N and the short timescale determined by τ_0, which are corresponding to the organic compounds that have the highest and lowest effective activation energy, respectively. Here, I perform asymptotic analyses for $B(t)$ in three regimes of degradation time t: short (i.e., $t \ll \tau_0$), intermediate (i.e., $\tau_0 \ll t \ll \tau_N$), and long (i.e., $\tau_N \ll t$). In the short-time regime, $t/\tau_N \ll t/\tau_0 \ll 1$, under which an asymptotic expansion[72] of Eq. (8) leads to

$$B(t) \simeq 1 - \frac{t}{\tau_0}\frac{RT}{\epsilon_{max}}\left[1 - \exp\left(-\frac{\epsilon_{max}}{RT}\right)\right], \quad \tau_0 \gg t. \quad (22)$$

This indicates that the preservation efficiency slightly decreases as degradation time increases in this short-time regime. When degradation time t is very short, Eq. (22) implies

$$B(t) \simeq 1 \text{ as } t \to 0. \quad (23)$$

In the intermediate-time regime, $t/\tau_N \ll 1 \ll t/\tau_0$, under which an asymptotic expansion[72] of Eq. (8) leads to

$$B(t) \simeq 1 - 2.3\log_{10}\left(\frac{t}{\tau_0}\right)\frac{RT}{\epsilon_{max}}, \quad \tau_0 \ll t \ll \tau_N. \quad (24)$$

In oxic environments (i.e., $t = t_{O_2}$), I obtain Eq. (9). In the long-time regime, $1 \ll t/\tau_N \ll t/\tau_0$, under which an asymptotic expansion[72] of Eq. (8) leads to

$$B(t) \simeq \frac{\tau_N}{t}\frac{RT}{\epsilon_{max}}\exp\left(-\frac{t}{\tau_N}\right), \quad t \gg \tau_N. \quad (25)$$

In this case, $B(t)$ is close to 0, indicateing that almost all organic matter is completely remineralized when the degradation time is sufficiently long:

$$B(t) \simeq 0 \text{ as } t \to \infty. \quad (26)$$

The average age of an organic-matter ensemble. As discussed in the Results section, the probability density function of organic matter's age, $p(t)$, equals $|dB(t)/dt|$. Since $B(t)$ is a monotonically decreasing function of t, I have $dB(t)/dt < 0$. With Eq. (8), I obtain the average age (i.e., the average waiting time before degradation) of all organic compounds in the hierarchical ensemble:

$$\langle t \rangle = \int_0^\infty tp(t)dt = -\left([tB(t)]_{t=0}^\infty - \int_0^\infty B(t)dt\right) \propto \frac{RT}{\epsilon_{max}}(\tau_N - \tau_0). \quad (27)$$

By definition, $\tau_N = 1/\kappa_N$ and $\tau_0 = 1/\kappa_0$. With the definition of effective degradation rate constant (i.e., $\kappa_i = (k_B T/\hbar)\exp[-\epsilon_i/(RT)]$), I obtain the relation between τ_N and τ_0:

$$\tau_N = \tau_0 \prod_{j=1}^{i} \exp\left(\frac{E_j}{RT}\right) = \tau_0 \exp\left(\frac{\epsilon_{max}}{RT}\right) \quad (28)$$

where E_j is the activation energy of the j-th reaction in the degradation continuum and is defined by Eq. (6). Then Eqs. (27) and (28) together give

$$\langle t \rangle \propto \frac{\exp(\epsilon_{max}/RT) - 1}{\epsilon_{max}/RT}\tau_0$$
$$= \left(\frac{RT}{\epsilon_{max}}\right)\left[1 + \left(\frac{\epsilon_{max}}{RT}\right) + \frac{1}{2}\left(\frac{\epsilon_{max}}{RT}\right)^2 + \frac{1}{6}\left(\frac{\epsilon_{max}}{RT}\right)^3 + \cdots - 1\right]\tau_0$$
$$= \left[1 + \frac{1}{2}\left(\frac{\epsilon_{max}}{RT}\right) + \frac{1}{6}\left(\frac{\epsilon_{max}}{RT}\right)^2 + \ldots\right]\tau_0 \quad (29)$$
$$\propto \exp\left(\frac{\epsilon_{max}}{RT}\right)\tau_0.$$

This shows that the average age, $\langle t \rangle$, monotonically increases with the maximum effective activation energy.

Power-law degradation behavior. To calculate the average degradation rate constant of all organic compounds in the ensemble, $K(t)$, I substitute $G(t) = G_0 B(t)$ and Eq. (8) into $dG(t)/dt = -K(t)G(t)$ and obtain

$$K(t) = -\frac{1}{G(t)}\frac{dG(t)}{dt}$$
$$= -\left(G_0\frac{RT}{\epsilon_{max}}\left[\text{Ei}\left(\frac{t}{\tau_N}\right) - \text{Ei}\left(\frac{t}{\tau_0}\right)\right]\right)^{-1} \cdot \left(G_0\frac{RT}{\epsilon_{max}}\right) \cdot \frac{d}{dt}\left[\text{Ei}\left(\frac{t}{\tau_N}\right) - \text{Ei}\left(\frac{t}{\tau_0}\right)\right].$$
$$= \left[\text{Ei}\left(\frac{t}{\tau_N}\right) - \text{Ei}\left(\frac{t}{\tau_0}\right)\right]^{-1} \cdot \left[\exp\left(-\frac{t}{\tau_N}\right) - \exp\left(-\frac{t}{\tau_0}\right)\right]\frac{1}{t}. \quad (30)$$

I consider organic matter degradation during a time interval between two extreme timescales – that is, $\tau_0 \ll t \ll \tau_N$. This condition implies

$$\text{Ei}\left(\frac{t}{\tau_0}\right) \ll \text{Ei}\left(\frac{t}{\tau_N}\right) \quad \text{and} \quad \exp\left(-\frac{t}{\tau_0}\right) \ll \exp\left(-\frac{t}{\tau_N}\right). \quad (31)$$

Eqs. (30) and (31) together give

$$K(t) = \left[\text{Ei}\left(\frac{t}{\tau_N}\right)\right]^{-1}\left[\exp\left(-\frac{t}{\tau_N}\right)\right]\frac{1}{t} \quad (32)$$

which is equivalent to Eq. (11).

Data availability
Data sharing not applicable to this article as no datasets were generated during the current study.

References
1. Galvez, M. E., Fischer, W. W., Jaccard, S. L. & Eglinton, T. I. Materials and pathways of the organic carbon cycle through time. *Nat. Geosci.* **13**, 535–546 (2020).
2. Hayes, J. M. & Waldbauer, J. R. The carbon cycle and associated redox processes through time. *Philosophical Trans. Royal Soc. B: Biol. Sci.* **361**, 931–950 (2006).
3. Forney, D. C. & Rothman, D. H. Common structure in the heterogeneity of plant-matter decay. *J. Royal Soc. Inter.* **9**, 2255–2267 (2012).
4. Kothawala, D. N., Kellerman, A. M., Catalán, N. & Tranvik, L. J. Organic matter degradation across ecosystem boundaries: The need for a unified conceptualization. *Trends Ecol. Evol.* (2020).
5. Sarmiento, J. L. *Ocean Biogeochemical Dynamics* (Princeton University Press, 2013).
6. Burdige, D. J. *Geochemistry of Marine Sediments* (Princeton University Press, 2021).
7. Jannasch, H. W. The microbial turnover of carbon in the deep-sea environment. *Global Planet. Chan.* **9**, 289–295 (1994).
8. Middelburg, J. J. Escape by dilution. *Science* **348**, 290–290 (2015).
9. Arrieta, J. M. et al. Dilution limits dissolved organic carbon utilization in the deep ocean. *Science* **348**, 331–333 (2015).
10. Keil, R. G. & Mayer, L. M. Mineral matrices and organic matter. In Holland, H. D. & Turekian, K. K. (eds.) *Treatise on Geochemistry*, vol. 12, 337-359 (Elsevier, Oxford, 2014), 2 edn.
11. Kleber, M. et al. Dynamic interactions at the mineral-organic matter interface. *Nat. Rev. Earth Env.* **2**, 402–421 (2021).
12. Bethke, C. M., Sanford, R. A., Kirk, M. F., Jin, Q. & Flynn, T. M. The thermodynamic ladder in geomicrobiology. *Am. J. Sci.* **311**, 183–210 (2011).

13. Westrich, J. T. & Berner, R. A. The role of sedimentary organic matter in bacterial sulfate reduction: The *G* model tested. *Limnolo. Oceanography* **29**, 236–249 (1984).

14. Middelburg, J. J. A simple rate model for organic matter decomposition in marine sediments. *Geochimica et Cosmochimica Acta* **53**, 1577–1581 (1989).

15. Boudreau, B. P. & Ruddick, B. R. On a reactive continuum representation of organic matter diagenesis. *Am. J. Sci.* **291**, 507–538 (1991).

16. Rothman, D. H. & Forney, D. C. Physical model for the decay and preservation of marine organic carbon. *Science* **316**, 1325–1328 (2007).

17. Polimene, L. et al. Modelling marine DOC degradation time scales. *Natl. Sci. Rev.* **5**, 468–474 (2018).

18. Arndt, S. et al. Quantifying the degradation of organic matter in marine sediments: A review and synthesis. *Earth-Sci. Rev.* **123**, 53–86 (2013).

19. LaRowe, D. E. & Van Cappellen, P. Degradation of natural organic matter: A thermodynamic analysis. *Geochimica et Cosmochimica Acta* **75**, 2030–2042 (2011).

20. Forney, D. & Rothman, D. Inverse method for estimating respiration rates from decay time series. *Biogeosciences* **9**, 3601–3612 (2012).

21. Westrich, J. T. & Berner, R. A. The effect of temperature on rates of sulfate reduction in marine sediments. *Geomicrobiol. J.* **6**, 99–117 (1988).

22. Craine, J. M., Fierer, N. & McLauchlan, K. K. Widespread coupling between the rate and temperature sensitivity of organic matter decay. *Nat. Geosci.* **3**, 854–857 (2010).

23. Lønborg, C., Álvarez-Salgado, X. A., Letscher, R. T. & Hansell, D. A. Large stimulation of recalcitrant dissolved organic carbon degradation by increasing ocean temperatures. *Front. Marine Sci.* **4**, 436 (2018).

24. Dittmar, T. et al. Enigmatic persistence of dissolved organic matter in the ocean. *Nat. Rev. Earth Env.* **2**, 570–583 (2021).

25. Kellerman, A. M., Kothawala, D. N., Dittmar, T. & Tranvik, L. J. Persistence of dissolved organic matter in lakes related to its molecular characteristics. *Nat. Geosci.* **8**, 454–457 (2015).

26. Hawkes, J. A., Patriarca, C., Sjöberg, P. J., Tranvik, L. J. & Bergquist, J. Extreme isomeric complexity of dissolved organic matter found across aquatic environments. *Limnol. Oceanography Lett.* **3**, 21–30 (2018).

27. Sobek, S. et al. Organic carbon burial efficiency in lake sediments controlled by oxygen exposure time and sediment source. *Limnology and Oceanography* **54**, 2243–2254 (2009).

28. Hartnett, H. E., Keil, R. G., Hedges, J. I. & Devol, A. H. Influence of oxygen exposure time on organic carbon preservation in continental margin sediments. *Nature* **391**, 572–575 (1998).

29. Zhang, S. et al. The oxic degradation of sedimentary organic matter 1400 Ma constrains atmospheric oxygen levels. *Biogeosciences* **14**, 2133–2149 (2017).

30. Middelburg, J. J., Vlug, T. & van der Nat, F. J. W. Organic matter mineralization in marine systems. *Global Planet Chan.* **8**, 47–58 (1993).

31. Beulig, F., Røy, H., Glombitza, C. & Jørgensen, B. B. Control on rate and pathway of anaerobic organic carbon degradation in the seabed. *Proc. Natl. Acad. Sci.* **115**, 367–372 (2018).

32. Katsev, S. & Crowe, S. A. Organic carbon burial efficiencies in sediments: The power law of mineralization revisited. *Geology* **43**, 607–610 (2015).

33. Eyring, H. The activated complex in chemical reactions. *J. Chem. Phys.* **3**, 107–115 (1935).

34. Laidler, K. J. & King, M. C. The development of transition-state theory. *J. Phys. Chem. A* **87**, 2657–2664 (1983).

35. Ross, J. & Vlad, M. O. Nonlinear kinetics and new approaches to complex reaction mechanisms. *Ann. Rev. Phys. Chem.* **50**, 51–78 (1999).

36. Plonka, A. *Dispersive Kinetics* (Springer Science & Business Media, 2013).

37. Montroll, E. W. & Shlesinger, M. F. On 1/*f* noise and other distributions with long tails. *Proc. Natl. Acad. Sci.* **79**, 3380–3383 (1982).

38. Amir, A., Oreg, Y. & Imry, Y. On relaxations and aging of various glasses. *Proc. Natl. Acad. Sci.* **109**, 1850–1855 (2012).

39. Mostovaya, A., Hawkes, J. A., Koehler, B., Dittmar, T. & Tranvik, L. J. Emergence of the reactivity continuum of organic matter from kinetics of a multitude of individual molecular constituents. *Env. Sci. Technol.* **51**, 11571–11579 (2017).

40. Arnosti, C., Reintjes, G. & Amann, R. A mechanistic microbial underpinning for the size-reactivity continuum of dissolved organic carbon degradation. *Marine Chemistry* **206**, 93–99 (2018).

41. Gudasz, C. et al. Temperature-controlled organic carbon mineralization in lake sediments. *Nature* **466**, 478–481 (2010).

42. Zonneveld, K. A. et al. Selective preservation of organic matter in marine environments; processes and impact on the sedimentary record. *Biogeosciences* **7**, 483–511 (2010).

43. Sobek, S., Zurbrügg, R. & Ostrovsky, I. The burial efficiency of organic carbon in the sediments of Lake Kinneret. *Aqua. Sci.* **73**, 355–364 (2011).

44. Sobek, S., Anderson, J. N., Bernasconi, S. M. & Del Sontro, T. Low organic carbon burial efficiency in arctic lake sediments. *J. Geophys. Res.: Biogeosci.* **119**, 1231–1243 (2014).

45. Turner, R. E., Rabalais, N. N. & Justić, D. Trends in summer bottom-water temperatures on the northern Gulf of Mexico continental shelf from 1985 to 2015. *PLoS One* **12**, e0184350 (2017).

46. Mayer, L. M. The inertness of being organic. *Marine Chem.* **92**, 135–140 (2004).

47. Lane, N. & Martin, W. The energetics of genome complexity. *Nature* **467**, 929–934 (2010).

48. LaRowe, D. E., Dale, A. W., Amend, J. P. & Van Cappellen, P. Thermodynamic limitations on microbially catalyzed reaction rates. *Geochimica et Cosmochimica Acta* **90**, 96–109 (2012).

49. Hoffmann, R., Minkin, V. I. & Carpenter, B. K. et al. Ockham's razor and chemistry. *Int. J. Philo. Chem.* **3**, 3–28 (1997).

50. Jeffreys, H. *The Theory of Probability* (Oxford University Press, 1998).

51. Oreskes, N., Shrader-Frechette, K. & Belitz, K. Verification, validation, and confirmation of numerical models in the Earth sciences. *Science* **263**, 641–646 (1994).

52. Jiao, N. et al. Microbial production of recalcitrant dissolved organic matter: Long-term carbon storage in the global ocean. *Nature Rev. Microbiol.* **8**, 593–599 (2010).

53. Lennartz, S. T. & Dittmar, T. Controls on turnover of marine dissolved organic matter-testing the null hypothesis of purely concentration-driven uptake: Comment on Shen and Benner, "Molecular properties are a primary control on the microbial utilization of dissolved organic matter in the ocean". *Limnol. Oceanography* **67**, 673–679 (2022).

54. Battin, T. J. et al. The boundless carbon cycle. *Nat. Geosci.* **2**, 598–600 (2009).

55. Basile-Doelsch, I., Balesdent, J. & Pellerin, S. Reviews and syntheses: The mechanisms underlying carbon storage in soil. *Biogeosciences* **17**, 5223–5242 (2020).

56. Lehmann, J. & Kleber, M. The contentious nature of soil organic matter. *Nature* **528**, 60–68 (2015).

57. Worrall, F., Burt, T. & Shedden, R. Long term records of riverine dissolved organic matter. *Biogeochemistry* **64**, 165–178 (2003).

58. Peralta-Maraver, I. et al. The riverine bioreactor: An integrative perspective on biological decomposition of organic matter across riverine habitats. *Sci. Total Env.* **772**, 145494 (2021).

59. Dauwe, B. & Middelburg, J. J. Amino acids and hexosamines as indicators of organic matter degradation state in North Sea sediments. *Limnol. Oceanography* **43**, 782–798 (1998).

60. Cowie, G. L. & Hedges, J. I. Sources and reactivities of amino acids in a coastal marine environment. *Limnol. Oceanography* **37**, 703–724 (1992).

61. Wei, J.-E. et al. Amino acids and amino sugars as indicators of the source and degradation state of sedimentary organic matter. *Marine Chem.* **230**, 103931 (2021).

62. Badii, R. *Complexity: Hierarchical Structures and Scaling in Physics* (Cambridge University Press, 1997).

63. Zheng, Y., Yanful, E. K. & Bassi, A. S. A review of plastic waste biodegradation. *Crit. Rev. Biotechnol.* **25**, 243–250 (2005).

64. Chen, C.-C., Dai, L., Ma, L. & Guo, R.-T. Enzymatic degradation of plant biomass and synthetic polymers. *Nat. Rev. Chemistry* **4**, 114–126 (2020).

65. Lenton, T. M., Daines, S. J. & Mills, B. J. COPSE reloaded: An improved model of biogeochemical cycling over Phanerozoic time. *Earth-Sci. Rev.* **178**, 1–28 (2018).

66. Ozaki, K., Cole, D. B., Reinhard, C. T. & Tajika, E. CANOPS-GRB v1.0: A new Earth system model for simulating the evolution of ocean–atmosphere chemistry over geologic timescales. *Geosci. Model Dev.* **15**, 7593–7639 (2022).

67. Kump, L. R. & Arthur, M. A. Interpreting carbon-isotope excursions: Carbonates and organic matter. *Chem. Geol.* **161**, 181–198 (1999).

68. Grotzinger, J. P., Fike, D. A. & Fischer, W. W. Enigmatic origin of the largest-known carbon isotope excursion in Earth's history. *Nat. Geosci.* **4**, 285–292 (2011).

69. Alcott, L. J., Mills, B. J. & Poulton, S. W. Stepwise Earth oxygenation is an inherent property of global biogeochemical cycling. *Science* **366**, 1333–1337 (2019).

70. Shang, H., Rothman, D. H. & Fournier, G. P. Oxidative metabolisms catalyzed Earth's oxygenation. *Nat. Commun.* **13**, 1–9 (2022).

71. Knapp, A. W. *Basic Real Analysis* (Springer Science & Business Media, 2007).

72. Bleistein, N. & Handelsman, R. A. *Asymptotic Expansions of Integrals* (Ardent Media, 1975).

Competing interests

The author declares no competing interests.

Additional information

Supplementary information The online version contains supplementary material available at https://doi.org/10.1038/s43247-022-00667-4.

Correspondence and requests for materials should be addressed to Haitao Shang.

Peer review information *Communications Earth & Environment* thanks Jack Middelburg, Christoph Voelker and the other, anonymous, reviewer(s) for their contribution to the peer review of this work. Primary Handling Editors: Joshua Dean and Clare Davis. Peer reviewer reports are available.

Reprints and permission information is available at http://www.nature.com/reprints

Publisher's note Springer Nature remains neutral with regard to jurisdictional claims in published maps and institutional affiliations.

COMMENT

Unified prediction of organic matter preservation and degradation

Jack J. Middelburg [1✉]

A mechanistic and predictive hierarchical model explains observed organic carbon burial efficiencies and degradation kinetics, and reveals that upper and lower limits of organic matter activation energies are key to predicting organic matter preservation and degradation rates.

Organic matter cycling forms an important part of the global carbon cycle and has been studied for many decades across multiple environments. Organic matter is consumed by microbes and animals for energy and biomass production, and through this process of mineralization, inorganic carbon and nutrients are released that sustain primary production and biogeochemical cycles. Although typically less than 1% of organic matter ultimately avoids mineralization, its accumulation in soils and sediments is an important long-term carbon sink. The reactivity and persistence of organic matter vary greatly and understanding what controls preservation and degradation rates has proven a challenge. Although degradation and preservation are two sides of the same coin, many studies focus on one or the other and rarely consider both dissolved and particulate forms. Writing in *Communications Earth & Environment*, Shang[1] presents a novel unified model that simultaneously predicts bulk organic matter preservation and degradation in aquatic systems.

Organic matter (OM) preservation and degradation is governed by multiple factors relating to OM chemistry, environmental conditions and the biological actors causing OM breakdown[2]. Natural OM is a heterogenous mixture of thousands of organic compounds that differ in composition, structure, origin, thermodynamic properties, degradation history, and how they interact with other molecules and minerals. Such factors influence degradability, with different molecules being preferentially consumed or preserved. This chemical view has its shortcomings, however, as OM preservation and degradation rates and pathways are also governed by multiple physical and chemical properties of the environment, including oxygen and nutrient availability, and temperature. In addition, organisms have specific traits and machinery to produce and consume OM and so the number, diversity and identity of consumers also play a major role. Accordingly, any generic model for OM processing should incorporate not only the heterogeneity in OM composition, but also the environmental conditions and heterotrophic community composition and functioning[3,4].

In their article, Shang[1] presents a new kinetic model of OM degradation and preservation, inspired by (quantum) statistical theory, that is mechanistic and predictive, which sets it apart from previous empirical and phenological models. Crucially, Shang's model quantitatively predicts both the observed logarithmic relation between organic carbon burial in sediments and oxygen exposure time[5] as well as empirical power-law degradation kinetics[6]. As such, Shang's hierarchical model unites OM preservation efficiencies and degradation rate patterns in a single model (Fig. 1). The model also predicts that more recalcitrant OM has a higher activation energy, which is consistent with observations[7]. Moreover, the upper and lower limits of OM activation energies are identified as key parameters to predict OM preservation and degradation rates over a wide range. This mechanistic incorporation of temperature sensitivity in the hierarchical model will be instrumental to further our knowledge on how OM preservation and degradation will respond to projected changes in temperature.

[1] Department of Earth Sciences, Utrecht University, Princetonlaan 8A, 3584 CD Utrecht, The Netherlands. ✉email: j.b.m.middelburg@uu.nl
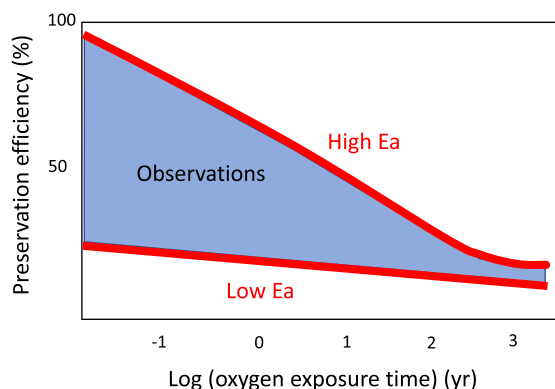
Fig. 1 Predicting organic matter preservation and degradation.
Theoretical predictions (red lines) of the relationship between organic matter preservation efficiency and oxygen-exposure time encompass observations. The upper and lower limit are set by the organic matter activation energies (adapted from ref. [1]).

The hierarchical model predictions should be tested with measurable OM reactivity proxies such as the amino acid degradation index[8] and serial oxidation inferred activation energies[9]. Shang's model is predictive but rooted in traditional first-order kinetic models that do not explicitly resolve consumer communities and their metabolism. In contrast, a recently proposed quantitative model for OM accumulation that explicitly resolved the ecological dynamics of the consumers combined the stochastic release of multiple pools of OM with microbial uptake by a community of specialist and generalist consumers[4]. Although both models are generic and largely consistent with observations, they differ in basic design, that is, geochemical kinetics versus ecological dynamics as well as in their overall goals: one seeks to predict OM degradation rates and preservation whereas the other was built to explain the accumulation of dissolved OM. Integration of these two approaches would be the logical next step towards a unified theory and predictive model of OM degradation and preservation across ecosystems and covering multiple timescales.

The unified model of Shang[1] shows that organic matter in aquatic systems is broken down in a hierarchical ensemble, involving a decrease in effective kinetic barriers. Through incorporating the temperature sensitivity of organic matter degradation, we can better understand and predict future changes to this globally important carbon pool under future warming.

References

1. Shang, H. A generic hierarchical model of organic matter degradation and preservation in aquatic systems. *Commun. Earth Environ.* https://doi.org/10.1038/s43247-022-00667-4 (2023).
2. Middelburg, J. J. & Meysman, F. J. R. Burial at sea. *Science* **316**, 1294–1295 (2007).
3. Kothawala, D. N. et al. Organic matter degradation across ecosystem boundaries: the need for a unified conceptualization. *Trends Ecol. Evol.* **36**, 113–122 (2021).
4. Zakem, E. J. et al. A unified theory for organic matter accumulation. *Proc. Natl. Acad. Sci. USA* **118**, 1–8 (2021).
5. Hartnett, H. E. et al. Influence of oxygen exposure time on organic carbon preservation in continental margin sediments. *Nature* **391**, 572–575 (1998).
6. Middelburg, J. J. A simple rate model for organic matter decomposition in marine sediments. *Geochim. Cosmochim. Acta* **53**, 1577–1581 (1989).
7. Westrich, J. T. & Berner, R. A. The effect of temperature on rates of sulfate reduction in marine sediments. *Geomicrobiol. J.* **6**, 99–117 (1988).
8. Dauwe, B. et al. Linking diagenetic alteration of amino acids and bulk organic matter reactivity. *Limnol. Oceanogr.* **44**, 1809–1814 (1999).
9. Hemingway, J. D. et al. Technical note: An inverse method to relate organic carbon reactivity to isotope composition from serial oxidation. *Biogeosciences* **14**, 5099–5114 (2017).

Competing interests
The author declares no competing interests.

Additional information
Correspondence and requests for materials should be addressed to Jack J. Middelburg.

Reprints and permission information is available at http://www.nature.com/reprints

Publisher's note Springer Nature remains neutral with regard to jurisdictional claims in published maps and institutional affiliations.

A Generic Hierarchical Model of Organic Matter Degradation and Preservation in Aquatic Systems – Supplementary Information –
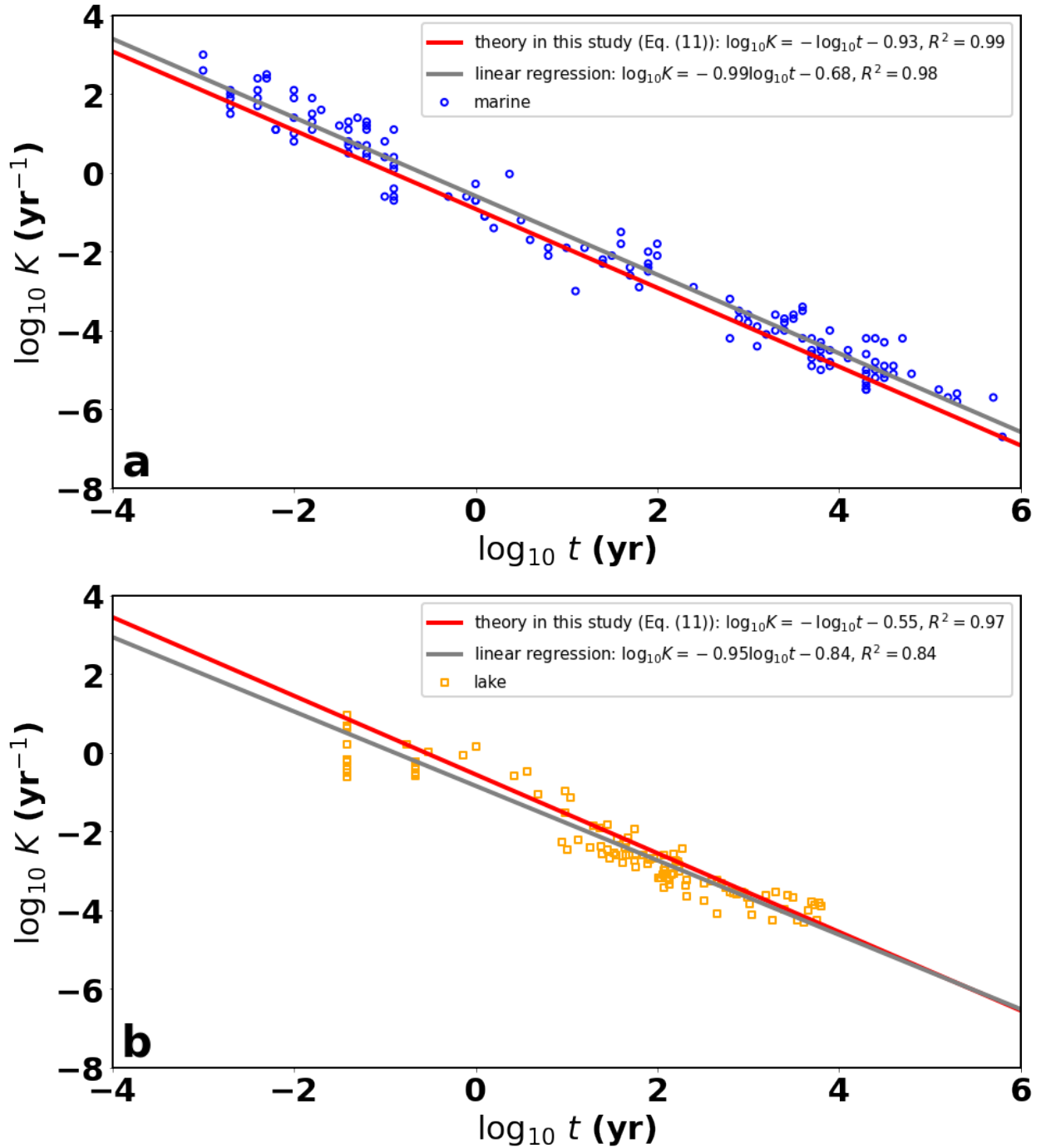
Haitao Shang[1] *

[1]Institute of Ecology and Evolution, University of Oregon, Eugene, OR, USA 97403

*To whom correspondence should be addressed; E-mail: htshang.research@gmail.com.

Contents

Supplementary Figure 1: **Theoretical predictions and field data for the power-law relation between organic carbon reactivity** (K) **and age** (t) **in marine and lake systems.** Blue circles in (a) represent data from marine systems[1] and orange squares in (b) represent data from lake systems[2]. Red straight lines in (a) and (b) represent theoretical approximations of Eq. (11) for the data from marine and lake systems, respectively. Grey straight lines in (a) and (b) represent linear regression analyses of the data from marine and lake systems, respectively. R^2 represents the coefficient of determination.

Supplementary Table 1: **Activation energy of organic matter in marine and lake sediments.**

Activation energy (kJ/mol)	Environment	Reference
36 – 132	marine sediments	Westrich and Berner (1988)[3]
75 – 88	marine sediments	Mackin and Swider (1989)[4]
29 – 59	marine sediments	Kristensen et al.(1992)[5]
54 – 125	marine sediments	Middelburg et al. (1996)[6]
46 – 89	marine sediments	Weston and Joye (2005)[7]
50 – 130	marine sediments	Burdige (2011)[8]
62 – 125	lake sediments	Duci et al. (2010)[9]
45 – 64	lake sediments	Gudasz et al. (2015)[10]

Supplementary Table 2: **Parameter values estimated using the hierarchical model or linear regression for power-law relation** $\log K = -a \log t + b$ **on marine, lake, and combined datasets.**

	Marine dataset	Lake dataset	Combined dataset
Hierarchical model, a	1	1	1
Linear regression, a	0.99	0.95	1
Hierarchical model, b	-0.93	-0.55	-0.94
Linear regression, b	-0.68	-0.84	-0.64
Hierarchical model, R^2	0.99	0.97	0.98
Linear regression, R^2	0.98	0.84	0.96

Supplementary References

[1] Jack J Middelburg, Tom Vlug, F Jaco, and WA Van der Nat. Organic matter mineralization in marine systems. *Global and Planetary Change*, 8(1-2):47–58, 1993.

[2] Sergei Katsev and Sean A Crowe. Organic carbon burial efficiencies in sediments: The power law of mineralization revisited. *Geology*, 43(7):607–610, 2015.

[3] Joseph T Westrich and Robert A Berner. The effect of temperature on rates of sulfate reduction in marine sediments. *Geomicrobiology Journal*, 6(2):99–117, 1988.

[4] James E Mackin and Kenneth T Swider. Organic matter decomposition pathways and oxygen consumption in coastal marine sediments. *Journal of Marine Research*, 47(3):681–716, 1989.

[5] Erik Kristensen, Frede Østerguard Andersen, and Thomas Henry Blackburn. Effects of benthic macrofauna and temperature on degradation of macroalgal detritus: the fate of organic carbon. *Limnology and Oceanography*, 37(7):1404–1419, 1992.

[6] Jack J Middelburg, Gerard Klaver, Joop Nieuwenhuize, Annette Wielemaker, Wim de Haas, Tom Vlug, and F. Jaco WA van der Nat. Organic matter mineralization in intertidal sediments along an estuarine gradient. *Marine Ecology Progress Series*, 132:157–168, 1996.

[7] Nathaniel B Weston and Samantha B Joye. Temperature-driven decoupling of key phases of organic matter degradation in marine sediments. *Proceedings of the National Academy of Sciences*, 102(47):17036–17040, 2005.

[8] David J Burdige. Temperature dependence of organic matter remineralization in deeply-buried marine sediments. *Earth and Planetary Science Letters*, 311(3-4):396–410, 2011.

[9] Nguyen Thanh Duc, Patrick Crill, and David Bastviken. Implications of temperature and sediment characteristics on methane formation and oxidation in lake sediments. *Biogeochemistry*, 100(1):185–196, 2010.

[10] Cristian Gudasz, Sebastian Sobek, David Bastviken, Birgit Koehler, and Lars J Tranvik. Temperature sensitivity of organic carbon mineralization in contrasting lake sediments. *Journal of Geophysical Research: Biogeosciences*, 120(7):1215–1225, 2015.